Journal of Inflammation Research

Dovepress
Taylor & Francis Group

Open Access Full Text Article

ORIGINAL RESEARCH

Glyuranolide-Dependent Inhibition of NF-κB/Akt Pathways by Sini Decoction Enhances Caspase-3-Mediated Apoptosis in Colorectal Cancer

Lihao Shi[1,*], Ling Zhang[2,*], Jiaju Xu[2], Bing Guo[2]

[1]Cheeloo College of Medicine, Shandong University, Jinan, 250012, People's Republic of China; [2]Department of Medical Oncology, Taian City Central Hospital, Taian, 271000, People's Republic of China

*These authors contributed equally to this work

Correspondence: Lihao Shi, Cheeloo College of Medicine, Shandong University, Jinan, 250012, People's Republic of China, Tel +86-0537-2903975, Email lihao_shi_md@163.com

Introduction: Colorectal carcinoma (CRC) is a leading cause of gastrointestinal malignancy worldwide. Its development is closely linked to aberrant activation of NF-κB and Akt signaling pathways. This study aimed to evaluate the inhibitory effects of Compound Sini Decoction (SND), a traditional Chinese medicine, on CRC and clarify its molecular mechanisms.

Methods: An AOM/DSS-induced mouse CRC model was used to assess the in vivo effects of SND. Network pharmacology identified potential targets, while molecular docking and kinetic simulations evaluated binding interactions. In vitro, SND-containing mouse serum was applied to HCT116 and SW480 cells to examine proliferation, migration, apoptosis, ROS production, and signaling pathway modulation.

Results: SND significantly reduced tumor burden, alleviated symptoms, and decreased body weight loss in mice. Network analysis highlighted NFKB1, CASP3, and AKT1 as key targets, suggesting regulation of NF-κB, Caspase-3, and Akt pathways. In vitro, SND inhibited cell proliferation and migration, induced apoptosis, promoted ROS accumulation, suppressed NF-κB and AKT1 phosphorylation, and enhanced CASP3 cleavage. Molecular docking showed Glyuranolide had the strongest binding affinity, particularly with NFKB1 and AKT1, indicating it as a likely effector compound.

Conclusion: SND exerts anti-CRC effects through multi-target synergistic mechanisms involving NF-κB/Akt signaling and Caspase-3-mediated apoptosis. Glyuranolide may represent its key active molecule. These findings provide preliminary evidence supporting SND or its derivatives as potential candidates for precision CRC therapy and suggest a strategy to overcome resistance to single-target treatment. Further studies are warranted to confirm the clinical translational value of SND and the specific role of Glyuranolide.

Keywords: colorectal cancer, Sini decoction, network pharmacology, molecular dynamics simulation, glyuranolide

Introduction

As a foremost gastrointestinal malignancy, colorectal cancer (CRC) develops through neoplastic transformation of the colonic mucosal epithelium. Its pathogenesis involves a multistep cascade of molecular alterations, characterized by uncontrolled proliferation and malignant transformation of colonic epithelial cells.[1] Although the precise mechanisms underlying CRC development remain incompletely elucidated, accumulating evidence highlights the critical involvement of the NF-κB and Akt signaling pathways in tumor initiation and progression.[2,3]

NF-κB, a pivotal transcription factor, drives CRC progression by modulating inflammatory responses, suppressing apoptosis, and facilitating tumor invasion and metastasis.[4] Chronic inflammation induces persistent NF-κB activation, triggering the sustained release of pro-inflammatory cytokines and cumulative DNA damage. Furthermore, NF-κB upregulates anti-apoptotic proteins, enabling tumor cells to evade immune surveillance.[2,4] Concurrently, Akt, a core effector of the PI3K/Akt/mTOR pathway, accelerates tumor growth by enhancing cellular proliferation, inhibiting

Received: 31 July 2025
Accepted: 4 October 2025
Published: 8 October 2025

apoptosis, and reprogramming metabolic pathways toward aerobic glycolysis.[5,6] Critically, these two pathways exhibit extensive crosstalk: Akt phosphorylates IKK, thereby activating NF-κB, while NF-κB transcriptionally upregulates Akt expression, establishing a pro-tumorigenic feedforward loop.[4,5] Dysregulated NF-κB and Akt signaling not only directly fuel carcinogenesis but also confer resistance to targeted therapies, including EGFR inhibitors. Given their synergistic role in CRC, dual inhibition of NF-κB and Akt pathways has emerged as a promising therapeutic strategy.[7]

Caspase-3, a key executioner protease, is initially synthesized as an inactive zymogen (procaspase-3) and undergoes proteolytic cleavage to form activated caspase-3 (cleaved caspase-3) in response to apoptotic stimuli.[8] This activation represents the final commitment step in the apoptotic cascade, irreversibly executing programmed cell death through substrate cleavage. In CRC, cleaved caspase-3 serves as both a biomarker and functional mediator, influencing tumor progression, therapeutic sensitivity, and clinical outcomes. Its expression levels correlate with treatment response and may provide prognostic value in CRC management.[9]

Sini Decoction (SND), a classical Traditional Chinese Medicine formulation, has been clinically employed for centuries and comprises three principal medicinal components: Fuzi/aconite, Gancao/licorice, and Ganjiang/ginger rhizome.[10] Accumulating preclinical evidence indicates that SND possesses potent anti-inflammatory properties and demonstrates inhibitory effects on CRC metastasis.[11] Nevertheless, the precise molecular mechanisms underlying SND's anti-CRC activity remain incompletely characterized. A systematic investigation of SND's therapeutic potential and mode of action could provide a scientific foundation for its incorporation into modern precision oncology approaches for CRC treatment.

This study systematically investigates the anti-CRC mechanisms of SND through an integrated approach, aiming to Identify the bioactive constituents responsible for its therapeutic effects, Characterize the key molecular targets and signaling pathways modulated by SND, and Elucidate the precise mechanisms underlying its inhibitory effects on colorectal cancer progression.

Materials and Methods

Identification of Active Compounds in SND and Computational Target Profiling

Pharmacologically active compounds in SND were identified and analyzed via the TCMSP database (https://old.tcmsp-e.com/tcmsp.php), a validated platform for traditional Chinese medicine systems pharmacology research. All phytochemical constituents derived from the three herbal components were systematically evaluated. Screening parameters incorporated established pharmacokinetic thresholds, including oral bioavailability (OB) ≥30% and drug-likeness (DL) ≥0.18, to identify bioactive candidates.[12] Following compound identification, potential protein targets were predicted through the STRING database (version 11.5; http://www.string-db.org) using default interaction parameters.[13] All identified targets were annotated with official gene symbols via UniProt (www.uniprot.org) to ensure standardized nomenclature for subsequent pathway and network analyses.

Identification of Colorectal Cancer-Associated Molecular Targets

Potential CRC targets were compiled from DisGeNET and GeneCards databases using stringent gene-disease association scores (GDAS >0.3 in DisGeNET, relevance score >0.7 in GeneCards).[14]

Network Pharmacology

Potential SND targets against CRC were predicted using the Bioinformatics Online platform's network pharmacology module.[15] PPI networks (STRING database, high-confidence interactions ≥0.40) were subjected to graph-theoretical analysis in Cytoscape 3.8.0 using cytoHubba. Active ingredients were prioritized by their degree scores, reflecting their relative importance within the interaction network.[16]

Molecular Docking Preparation

The two-dimensional structural data of candidate ligands were acquired from the PubChem database. These structures underwent three-dimensional conformational optimization using ChemOffice 2022 (PerkinElmer) with output saved in

mol2 format. For receptor preparation, a high-resolution crystal structure of the target protein was retrieved from the RCSB Protein Data Bank (http://www.rcsb.org/) and processed using PyMOL to remove heteroatoms and phosphorylation modifications. Protein-ligand docking simulations were conducted using AutoDock Vina 1.5.6 (The Scripps Research Institute). Systematic structure preparation was performed through AutoDock Tools 1.5.7. The docking grid dimensions were carefully optimized to encompass the predicted binding site, with the most favorable binding pose selected based on calculated affinity scores (kcal/mol). Protein-ligand interactions were visualized and analyzed using Discovery Studio 2019. This integrated approach enabled systematic evaluation of the molecular interactions between SND-derived compounds and their putative protein targets.

Molecular Dynamics Simulation

All-atom molecular dynamics simulations were conducted using GROMACS 2023.2 (GROningen MAchine for Chemical Simulations).[17] Each complex was solvated in a cubic periodic boundary box with TIP3P water molecules and appropriate counterions to maintain system neutrality. The molecular dynamics simulations employed the Particle Mesh Ewald (PME) method with a 1.0 nm cutoff for long-range electrostatic interactions, while van der Waals interactions were similarly treated with a 1.0 nm cutoff distance, incorporating a switch function between 0.8–1.0 nm for smooth potential truncation, and utilized the Verlet neighbor list algorithm with a 1.2 nm update frequency and 0.005 kJ/mol/ps buffer tolerance to efficiently manage non-bonded interactions. The system underwent energy minimization followed by a two-phase equilibration protocol: (1) 50,000 steps of NVT (constant particle number, volume, and temperature) equilibration using the Berendsen thermostat (τ = 0.1 ps) at 300 K, and (2) 50,000 steps of NPT (constant particle number, pressure, and temperature) equilibration with the Berendsen barostat (τ = 0.1 ps) at 1 bar. Production simulations were subsequently conducted for 100 ns under isothermal-isobaric conditions (300 K, 1 bar) using the Verlet integration algorithm with a 2-fs time step.

Sini Decoction Preparation and Dosage Regimen

The study utilized Sini decoction prepared from certified finished drug product (Batch No. 031439, KO DA Pharmaceuticals Ltd)., manufactured in compliance with current Good Manufacturing Practice standards. For animal dosing, the human equivalent dose was calculated through standardized interspecies conversion following FDA Guidance for Industry (2019) on dose translation. Based on the manufacturer's recommended adult human dose of 12 g/day (60 kg body weight), the murine equivalent dose was derived using body surface area normalization with a conversion factor of 12.3 (Reagan-Shaw et al, 2008), resulting in a calculated daily dose of 0.4065 mg. This base dose was further adjusted according to individual animal body weights to maintain stable therapeutic concentrations throughout the study period.

Establishment of Colorectal Cancer Mouse Model and SND Treatment

C57BL/6 mice (20–23 g) were housed under SPF conditions and randomly divided into two groups: PBS-treated controls (WT) and SND-treated group (WTSND). Colorectal Cancer Mouse Model was induced by azoxymethane (10 mg/kg) followed by three cycles of 1.5% DSS in drinking water (7-day exposure per cycle, each followed by a 14-day recovery period). During recovery phases, the WTSND group received Sini Decoction via oral gavage every 48 hours, while the WT group received PBS. Mice were monitored twice weekly for disease activity (body weight, stool consistency, and fecal blood) and survival. After a final 7-day observation period, mice were euthanized for evaluation of colon lesions, tumor count, and histopathological analysis.

Preparation of Drug-Containing Serum

Administer the drug at the previously described doses for 7 consecutive days. After the last administration, collect the blood, let it stand for 30 minutes, centrifuge, separate the serum, filter and sterilize it, then aliquot and store at −80°C.

Cell Culture and Drug-Containing Serum Treatment

Human colorectal cancer cell lines HCT116 (TCHu 99) and SW480 (TCHu172) were purchased from the National Collection of Authenticated Cell Cultures (Shanghai, China). All cell lines were cultured and passed according to the

supplier's instructions. Control group (SW480, HCT116): Regular culture medium (containing 5% fetal bovine serum + 5% mouse-derived serum). SND group (SW480SND, HCT116SND): Add drug-containing serum to the culture medium (containing 5% fetal bovine serum + 5% drug-containing mouse-derived serum).

CCK-8 Cell Proliferation Assay Experiment

For temporal analysis, cells were distributed evenly across multiple 96-well plates and harvested at 24-hour intervals for subsequent assays. During the detection process, 10 μL of CCK-8 reagent (C0038, Beyotime) was added to each well. The plates were incubated for 1 hour at 37°C, and the absorbance at 450 nm (OD value) was measured using an enzyme reader.

Wound Healing Assay

A scratch was made using an aseptic pipette, ensuring that the scratch width was as consistent as possible. The plate was gently rinsed three times with PBS to remove detached cells. The medium without serum (or the medium containing the test drug) was added. The scratch area was photographed using a microscope at 0 hours and 24 hours. The area of the scratch width was measured using ImageJ software, and the Residual Wound Area Ratio (24-hour Area / 0-hour Area) was calculated.

Cell ROS Detection Experiment

According to the instructions of the reagent kit, dilute DCFH-DA (50101es01, Yeasen) in serum-free medium or PBS to a final concentration of 1 μM. Discard the original medium, add the working solution containing the probe (1 mL per well, 6-well plate), incubate at 37°C in the dark for 30 minutes. Wash the cells gently twice with pre-warmed PBS to remove the un-entered probe from the cells. Resuspend the cells in 200 μL PBS. Subsequently, intracellular ROS levels were measured using flow cytometry (BD FACSCanto II, BD Biosciences). The fluorescence intensity of FITC as recorded, and at least 10,000 events were collected for each sample. Data were analyzed using FlowJo software, and the mean fluorescence intensity was used as an indicator of relative ROS production in CRC cells.

Western Blotting

Proteins were extracted using RIPA buffer with protease/phosphatase inhibitors, quantified by BCA assay, separated by SDS-PAGE, and transferred to PVDF membranes for immunoblotting analysis. Membranes were blocked with 4% BSA in TBST for 1 h at room temperature to prevent non-specific binding, followed by overnight incubation at 4°C with the following primary antibodies: The following primary antibodies were used: phospho-Akt (Ser473; #4060), total Akt (#4691), phospho-NF-κB p65 (Ser536; #3033), total p65 (#8242), cleaved caspase-3 (#9664), and β-actin (#4970) (all 1:1000 dilution; Cell Signaling Technology).

Statistical Analysis

All quantitative data are expressed as mean ± standard deviation (SD) from at least three independent experiments. Statistical significance ($p<0.05$) was determined using two-tailed unpaired t-tests with Welch's correction (GraphPad Prism 9.0), following variance homogeneity verification by F-tests.

Results

SND Effectively Inhibits the Disease Severity of the Mouse Model of Colon Cancer Induced by AOM/DSS

Although previous scholars have already established subcutaneous tumor models to verify the significant positive effects of SND on colon tumors, to better simulate the physiological and pathological environment of colon cancer and to verify the therapeutic effect of SND on colon cancer, we constructed an AOM/DSS-induced colon cancer mouse model and intervened with SND from the first cycle. Consistent with the previous results, SND treatment of AOM/DSS model mice could effectively improve symptoms such as bloody stool and diarrhea, improve the disease activity, the percentage of weight loss in mice with colon cancer was also reduced (Figure 1A–C). And SND treatment reduces the number of colon

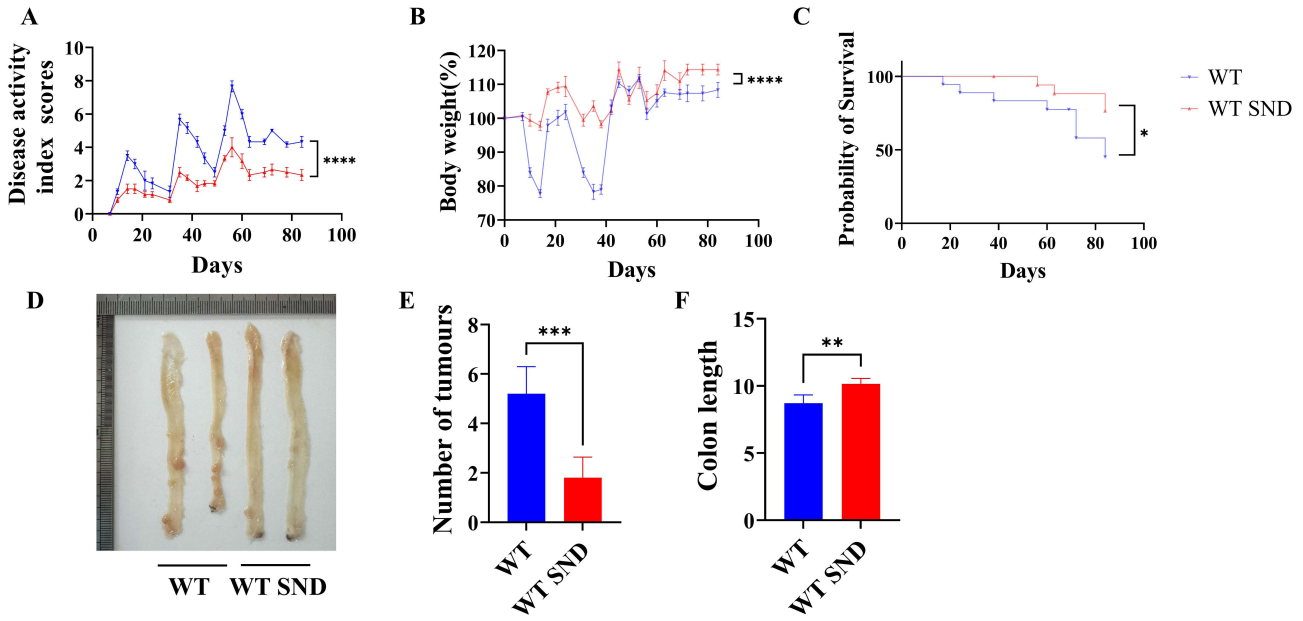

Figure 1 SND inhibited the progression of AOM/DSS-induced colorectal cancer in mice. Both groups of mice were subjected to the colon cancer model treatment as described earlier, using AOM/DSS. During the stabilization period, the WTSND group was given SND by gavage every two days, while the WT group was given PBS instead. (**A**) The DAI of mice was calculated twice weekly during the observation period. (**B**) Changes in mouse body weight were expressed as a percentage of the initial body weight at the start of the experiment, with weight measurements taken twice weekly. (**C**) Survival rates of mice in both groups during the observation period. (**D**) Representative macroscopic images of mouse colons were captured. (**E**) Tumors in the colons of mice in both groups were counted, and (**F**) mouse colon length was measured. *P < 0.05, **P < 0.01, ***P < 0.001, ****P < 0.0001.

tumors, alleviating the tumor burden of the mice, (Figure 1D–F). Overall, SND treatment can effectively alleviate colon cancer induced by AOM/DSS, which has aroused our interest in further studying its therapeutic mechanism.

Identification of Core Targets of SND in CRC: NFKB1, CASP3, and AKT1

To understand how SND exerts its anti-tumor effects, we first focused on its main components. Following the previously described methodology, we extracted 10, 85, and 3 active compounds from aconite, licorice, and ginger rhizome, respectively. Subsequently, we identified the corresponding target proteins for each compound and compiled a comprehensive list of potential targets. By cross-referencing these targets with known CRC-related pathogenic genes, we found that SND shares 229 potential targets with 1,404 CRC-associated genes (Figure 2A). To elucidate the interactions between SND and CRC, the PPI network was generated using the STRING database. The resulting network comprised 229 nodes and 5,419 edges (Figure 2B). Using Cytoscape, we identified the top 14 hub genes based on the following thresholds: Closeness > 0.00293, Betweenness > 192.6113537, and Degree > 47.32751092. After filtering, the core network was refined to 14 nodes and 90 edges, among which NFKB1, CASP3, and AKT1 emerged as the most prominent targets (Figure 2C). Since these genes are well-established central regulators of the NF-κB, CASP3-mediated apoptosis, and Akt signaling pathways, respectively, our results indicate that these pathways are most likely to be the key downstream mechanisms influenced by SND. Therefore, it is reasonable to infer that SND may exert its anti-CRC effects primarily through modulation of these three pathways.

SND Can Effectively Inhibit the Growth of Colon Cancer Cells

Given the positive effects of SND demonstrated in the mouse model of colon cancer, as well as the potential targets suggested by network pharmacology, we wondered whether SND could exhibit the same astonishing effect at the cellular level on colon cancer cells. And indeed, this was the case. To better simulate the effects of SND in the body, we added mouse drug-containing serum or drug-free serum to the normal culture medium to treat two types of colon cancer cells, to prove the effect of SND. We first used the CCK-8 method to detect the proliferation of colon cancer cells treated with mouse serum containing SND. The results showed that after treatment with serum containing SND, the proliferation of

https://doi.org/10.2147/JIR.S557303

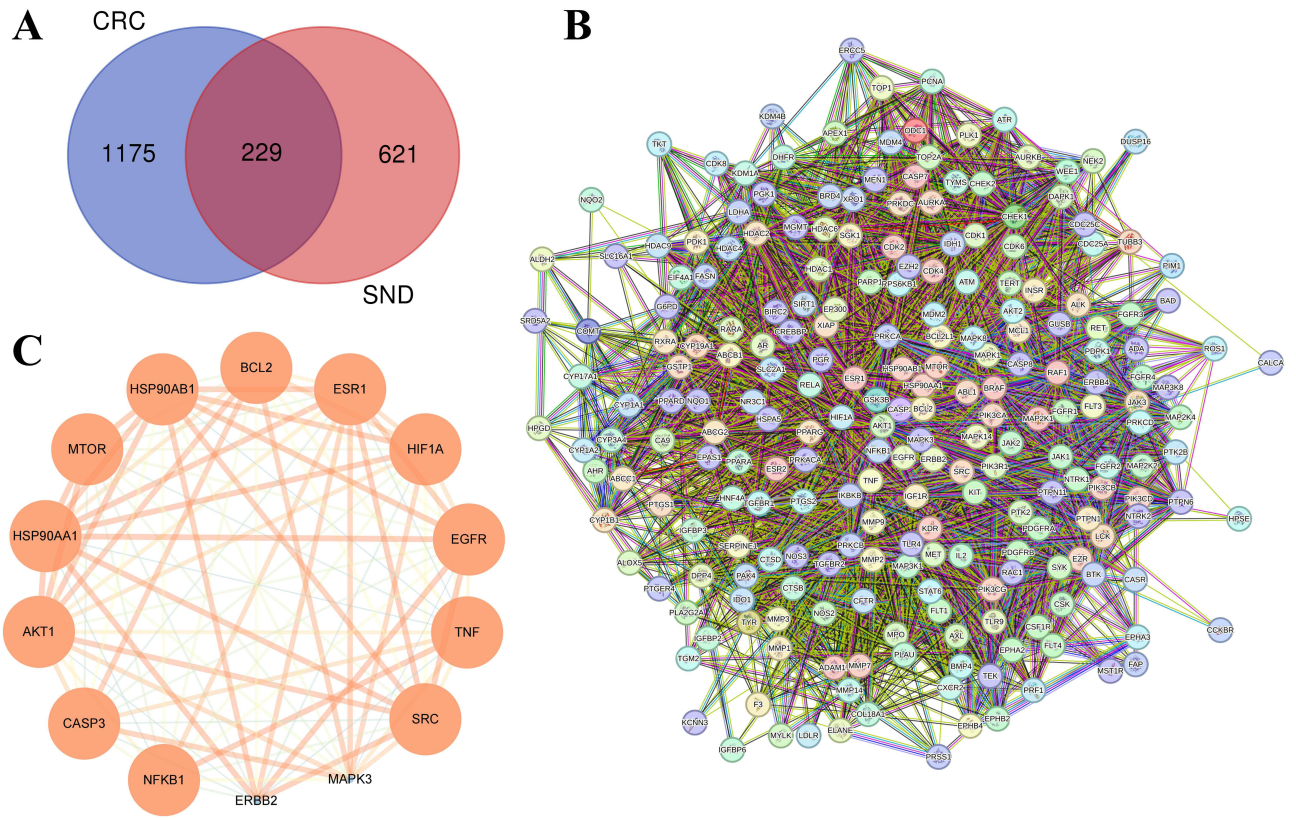

Figure 2 Protein interaction network of SND targets and core targets in UC therapy. (**A**) Venn diagram illustrating the 229 overlapping genes associated with CRC in SND therapy. (**B**) Protein interaction network in the STRING database, where SND shares 229 potential targets and 5,419 edges with 1,404 CRC-associated genes. (**C**) Analysis of the PPI network using Cytosccape software to illustrate the 14 key targets affected by SND in CRC therapy. Higher degree values are represented by colors closer to red.

HCT116 and SW480 colon cancer cells was successfully inhibited (Figure 3A and B). Further cell scratch experiments also indicated that SND significantly reduced the migration ability of the two types of colon cancer cells, suggesting its potential for long-term inhibition of tumor invasion (Figure 3C–F).

SND Inhibits NFKB1 and AKT1 and Regulates CASP3 Cleavage in Colon Cancer Cells

Given that reactive oxygen species (ROS) accumulation constitutes one of the key signaling events triggering apoptosis, we subsequently investigated whether SND treatment influences ROS levels within CRC cells. To further investigate the cellular state of colon cancer cells treated with SND serum, we used flow cytometry to detect the expression of ROS in these cells. The analysis results showed that SND treatment could significantly increase the expression of ROS in colon cancer cells (Figure 4A–D). It is well known that when ROS accumulates beyond the antioxidant capacity of cancer cells, it will cause irreversible oxidative damage, leading to the death of cancer cells. This mechanism is one of the core strategies of various anti-cancer therapies. We now suspect that after receiving treatment with SND serum, SND may somehow disrupt the normal proliferation activities of colon cancer cells and ultimately lead to their apoptosis. To prove our hypothesis, we subsequently conducted Western blot analysis to verify the targets suggested by network pharmacology. The results showed that SND reduced the phosphorylation of NF-κB and AKT1 in two types of colon cancer cells and increased the cleavage of CASP3 (Figure 4E–H). This indicates that SND may induce apoptosis of colon cancer cells through a triple synergistic mechanism and execute the apoptotic process. This multi-targeted action demonstrates the interesting potential of SND in treating colon cancer. This effect may synergistically overcome single-pathway resistance and provides potential candidate compounds for the development of new colon cancer treatment strategies. However, further verification is still required.

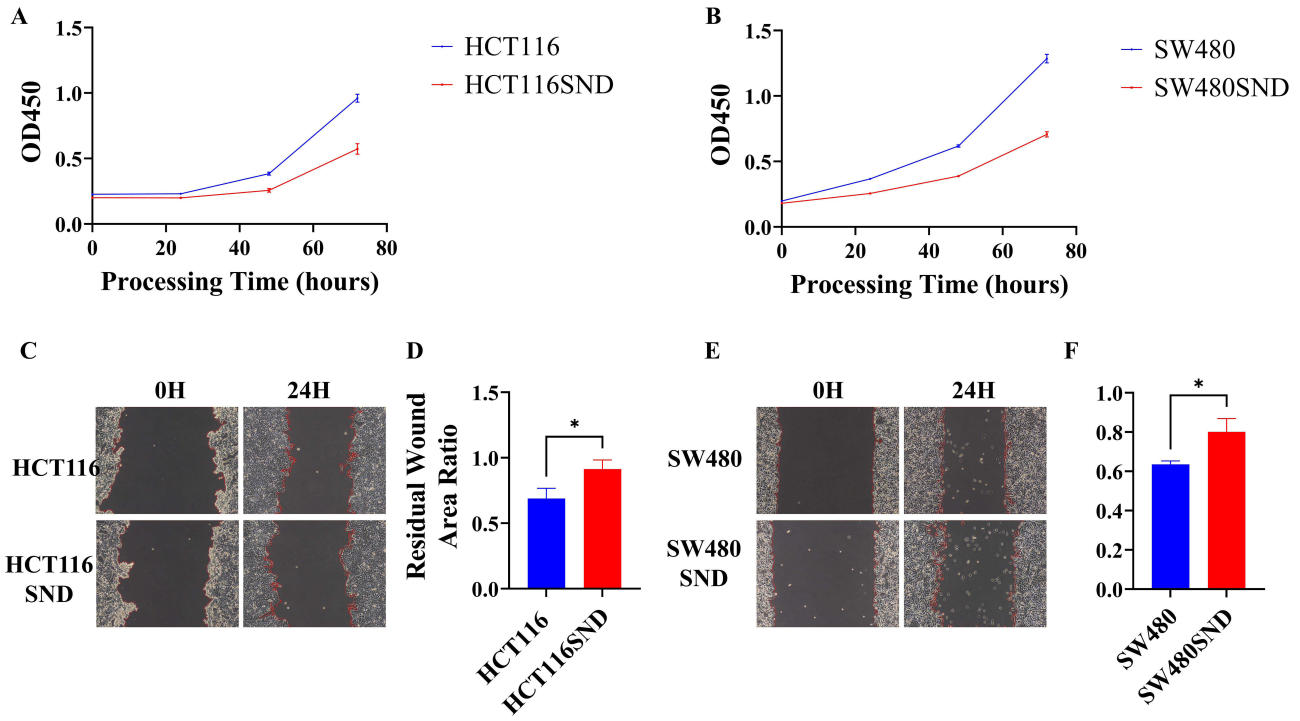

Figure 3 SND effectively inhibits the growth of colon cancer cells. In the control group (SW480, HCT116), conventional medium (5% normal animal serum + 5% control medium) was used. In the SND group (SW480SND, HCT116SND), drug-containing serum (5% normal animal serum + 5% drug-containing serum) was added to the culture medium. (**A** and **B**) The proliferation of HCT116 and SW480 colon cancer cells was successfully inhibited by treatment with serum containing SND, (**C** and **E**) which significantly reduced the migration ability of these two colon cancer cells in a cell scratch assay, and (**D** and **F**) the scratch areas of the two types of cells were recorded at 0 h and 24 h and Residual Wound Area Ratio (24-hour Area / 0-hour Area). *P < 0.05.

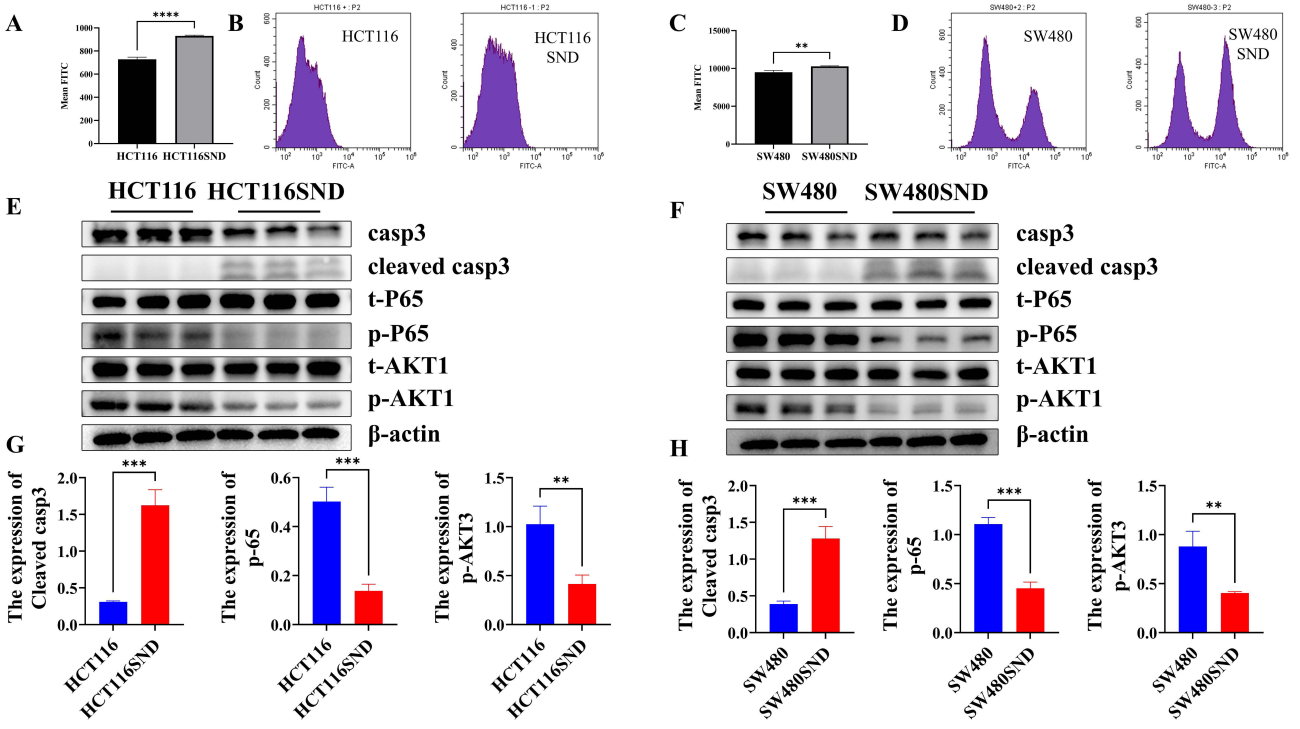

Figure 4 SND inhibits NFKB1 and AKT1 and regulates CASP3 cleavage in colon cancer cells. (**A** and **C**) SND treatment significantly increased the amount of ROS in colon cancer cells, and (**B** and **D**) representative images were selected. (**B** and **D**) Western blot analysis of NF-κB and AKT1 as well as CASP3 in two types of colon cancer cells treated with SND (**E** and **F**), using β-actin as (**G** and **H**) a reference and quantitatively analyzed. **P < 0.01, ***P < 0.001, ****P < 0.0001.

https://doi.org/10.2147/JIR.S557303

Effective Binding Between SND's Active Components and Core CRC Targets

To determine which bioactive compound in SND plays the anti-tumor role, we sorted all the active components based on their degree of centrality and selected the top 15 compounds. Subsequently, we conducted molecular docking simulations on these 15 compounds to evaluate their binding affinity and interaction patterns with the core CRC targets (NFKB1, CASP3, and AKT1) (Figure 5A). The analysis indicated that many compounds from different SND sources have strong potential for binding to NFKB1, CASP3, and AKT1, suggesting that they have direct regulatory effects on the key signaling pathways of colorectal cancer. It is particularly noteworthy that Glyuranolide exhibits a high binding ability to all three targets (NFKB1, CASP3, and AKT1) (Figure 5B–D). This compound was first discovered in 1989, but its role in anti-colon tumor has not yet been widely known.

Molecular Dynamics Simulation of Glyuranolide

To further verify the stability and binding behavior of the Glyuranolide active compound with the core targets of CRC (NFKB1, CASP3, AKT1), we conducted molecular dynamics (MD) simulations (100 ns). Root mean square deviation (RMSD) analysis assessed system stability by measuring atomic positional fluctuations from initial conformations. Lower RMSD values indicate greater structural stability. As shown in Figure 6A Among them, the RMSD value of the NFKB-Glyuranolide complex was lower. Therefore, the Glyuranolide small molecule showed higher stability when binding to the NFKB target protein. Radius of gyration (Rg) analysis revealed stable structural compactness for both AKT1-Glyuranolide and NF-κB-Glyuranolide complexes, with minimal fluctuations suggesting no significant expansion/contraction (Figure 6B). Solvent-accessible surface area (SASA) calculations further confirmed structural stability, as neither complex exhibited substantial surface area changes upon ligand binding (Figure 6C). Hydrogen bonds play an

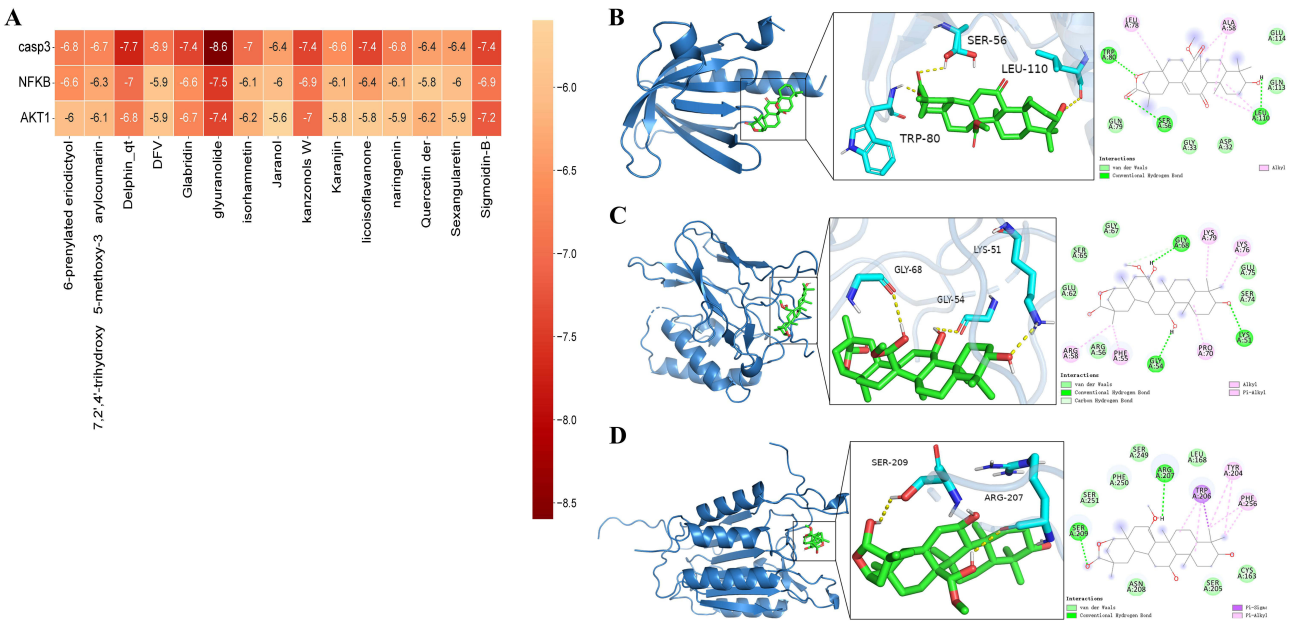

Figure 5 Effective binding of key active ingredients of SND to core CRC targets. (**A**) Molecular docking simulations of the top 15 compounds in SND with NFKB1, CASP3 and AKT1 are plotted in a heat map. The left side represents the target molecule, and the bottom side represents the name of each of the 15 active ingredients, and the stronger the binding ability, the closer to the red color, according to the marking on the right side, as reflected in the heat map. Molecular docking demonstration of Glyuranolide with three targets, NFKB1, CASP3 and AKT1. (**B**) TRP80, SER56, LEU110 residues on AKT1 receptor form hydrogen-bonding interaction force with glyuranolide, LEU78, ALA58, LEU110 residues on AKT1 receptor form hydrophobic interaction force with glyuranolide, and residues GLU114, GLN113, ASP32, and GLN72 on the AKT1 receptor form hydrophobic interactions with glyuranolide, and residues GLU114, GLN113, ASP32, and GLN72 on the AKT1 receptor form van der Waals interactions with glyuranolide. (**C**) Residues GLY68, LYS51, and GLY54 on the NFKB receptor form hydrogen bonding interaction force with glyuranolide, residues LYS79, LYS76, PRO70, PHE55, and ARG58 on the NFKB receptor form hydrophobic interaction force with glyuranolide, and GLU67 on the NFKB receptor, SER65, GLU62, ARG56, SER74, GLU75 residues on NFKB receptor formed van der Waals interaction force with glyuranolide. (**D**) Residues ARG207, SER209 on CASP3 receptor formed hydrogen bonding interaction force with glyuranolide, residues TYR204, PHE256, TRP206 on CASP3 receptor formed hydrophobic interaction force with glyuranolide, residues ASN208, SER205, CYS163, SER251, PHE251, and TRP206 on CASP3 receptor formed hydrophobic interaction force with glyuranolide. SER208, SER205, CYS163, SER251, PHE250, SER249, and LEU168 residues on CASP3 receptor form a van der Waals interaction with glyuranolide, and TRP206 residue on CASP3 receptor forms a Pi -Sigma interaction with glyuranolide.

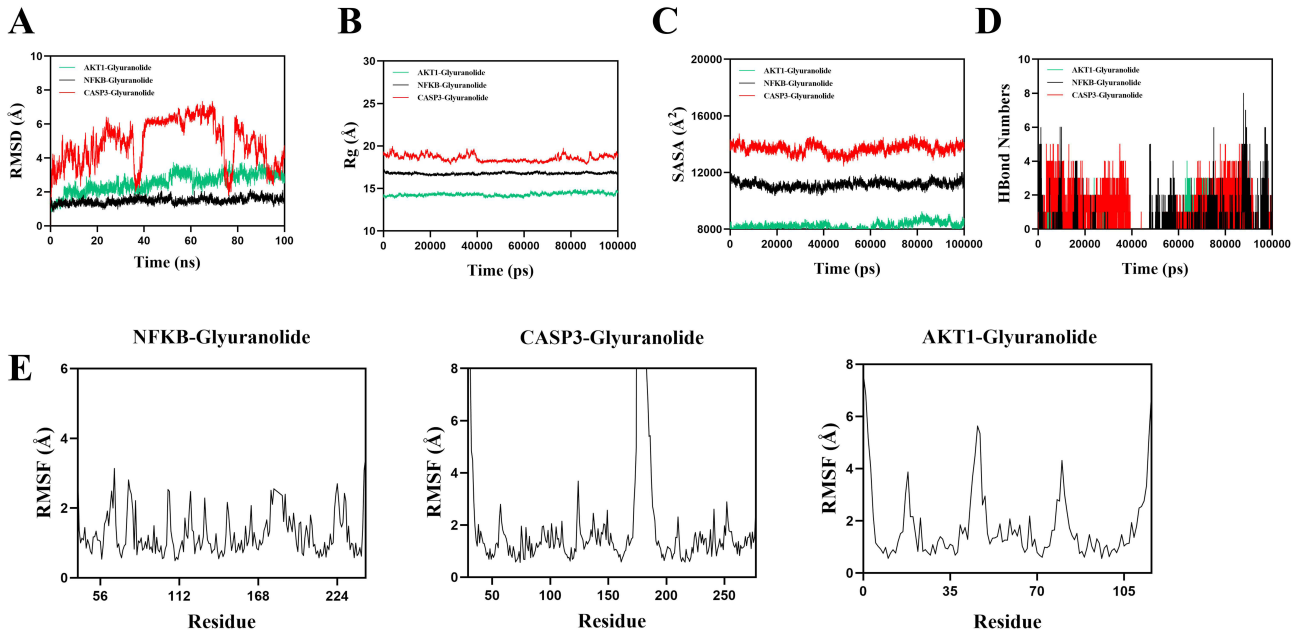

Figure 6 Glyuranolide - NFKB1, CASP3 and AKT1. Molecular dynamics simulations of the complexes. (**A**) RMSD values of the three complexes over time; (**B**) Rg values of the three complexes over time; (**C**) SASA values of the three complexes over time; (**D**) HBonds values of the three complexes over time; (**E**) RMSF values of the three complexes.

important role in the binding of ligands and proteins. The number of hydrogen bonds between the small molecule and the target protein during the kinetic process is shown in Figure 6D. The number of hydrogen bonds between the AKT1-Glyuranolide small molecule and the target protein ranged from 0 to 4, and in most cases, the complex had approximately 1 hydrogen bond. The number of hydrogen bonds between the NFKB-Glyuranolide small molecule and the target protein ranged from 0 to 8, and in most cases, the complex had approximately 1 hydrogen bond. This indicates that this ligand has a good hydrogen bond interaction with the target protein. The root mean square fluctuation (RMSF) can represent the flexibility of amino acid residues in proteins. As shown in Figure 6E, the RMSF values of the AKT1-Glyuranolide and NFKB-Glyuranolide complexes were relatively low (mostly below 3 A), so their flexibility was low, and their stability was high. In conclusion, the AKT1-Glyuranolide and NFKB-Glyuranolide complex systems were stable in binding, and the complexes had good hydrogen bond interactions. Therefore, the binding of the Glyuranolide small molecule to the AKT1 and NFKB target proteins was good.

Discussion

This study demonstrates that the Four-Counterflow Decoction (SND) can effectively alleviate the severity of the disease in the colon cancer mouse model induced by AOM/DSS. It not only verifies its anti-tumor effect but also reveals its multi-target mechanism through multi-omics and functional experiments. It is found that SND regulates core targets such as NFKB1, CASP3, and AKT1 to inhibit tumor growth, migration, and survival of colorectal cancer.

The AOM/DSS model simulates the process of inflammation-related colorectal cancer occurrence, confirming that SND can reduce the number of tumors, alleviate symptoms, and lower the proportion of weight loss in mice. This result is consistent with previous results of subcutaneous transplanted tumor models but further proves the therapeutic potential of SND in the inflammatory microenvironment.[11] However, its clinical translation still requires further pharmacokinetic and toxicity studies for support. SND is currently in clinical use in certain Asian countries, though its therapeutic effects have yet to extend into the field of cancer treatment. Numerous issues remain to be urgently addressed: what dosage of SND is required within the human body to achieve antitumor effects? As a medicinal agent, where should its appropriate application lie – in tumor prevention? Or in the early stages of tumors? Might it still prove effective in advanced stages of tumors? Furthermore, should SND demonstrate anti-timor efficacy, could Glyuranolide fully replicate these effects?

https://doi.org/10.2147/JIR.S557303

Future research should focus on identifying SND's precise active components and validating their efficacy. Through protein interaction (PPI) network analysis, we identified NFKB1, CASP3, and AKT1 as key targets, suggesting that the mechanism of SND may involve inhibiting the NF-κB pathway: reducing inflammation-driven tumor progression;[18] activating CASP3: promoting caspase-dependent apoptosis;[19] inhibiting AKT1: blocking survival signals and cell proliferation.[20] It is noteworthy that the synergistic regulation of these three pathways by SND may enable it to overcome the common resistance problems of single-targeted treatment. The serum of mice containing SND can inhibit the proliferation and migration of HCT116 and SW480 cells, consistent with the results in vivo. Mechanistically, SND induces the accumulation of reactive oxygen species, causing cancer cells to exceed their antioxidant capacity, leading to irreversible oxidative damage.[21] Western blot further confirms that SND can reduce the phosphorylation of NF-κB and AKT1 and promote the cleavage of CASP3, thereby inducing cancer cell apoptosis. Molecular docking and kinetic simulation revealed that Glyuranolide in licorice has high binding affinity with NFKB1, CASP3, and AKT1. MD simulation showed that the binding of Glyuranolide to NFKB1 is the most stable, while the unstable binding to CASP3 is unexpected and requires further study. Although this compound was discovered as early as 1989, its anti-colorectal cancer effect has not been widely recognized, and further research is warranted.[22]

Although molecular docking results in this study suggest **Glyuranolide** may be a key active component of SND, definitive confirmation ultimately requires direct functional experiments using pure Glyuranolide compounds, systematically comparing their effects with those of the whole SND formulation and other constituents. This represents the most significant future direction for this research and constitutes a critical challenge that must be addressed to advance the precision-oriented study of traditional Chinese medicinal formulas. We call upon and anticipate greater scholarly engagement in this field to collectively advance in-depth pharmacological mechanism research on such natural active monomers. Future research can focus on evaluating the safety and efficacy of SND for CRC patients and independently verifying the specific role of Glyuranolide; and exploring the synergistic effect of SND with conventional chemotherapy drugs.

Conclusion

SND may exert anti-CRC effects through a multi-target mechanism, with Glyuranolide being a potential key effector molecule. The ability of SND to regulate multiple pathways in a synergistic manner suggests its promise as a strategy to address the limitations of single-targeted treatment. Our findings provide preliminary evidence and a theoretical reference for the potential application of SND or its derivatives in precision tumor therapy.

Ethical Statement

This study was approved by the Research Ethics Committee of Tai'an Central Hospital (approval number 20220696). All animal procedures were carried out in accordance with China's regulations on laboratory animals and the institutional and national ethical guidelines for human data research, including confidentiality protection.

Author Contributions

All authors made a significant contribution to the work reported, whether that is in the conception, study design, execution, acquisition of data, analysis and interpretation, or in all these areas; took part in drafting, revising or critically reviewing the article; gave final approval of the version to be published; have agreed on the journal to which the article has been submitted; and agree to be accountable for all aspects of the work.

Funding

The authors declare that no funds, grants, or other support were received during the preparation of this manuscript.

Disclosure

The authors report no conflicts of interest in this work.

References

1. Benson AB, Venook AP, Adam M, et al. Colon Cancer, Version 3.2024, NCCN Clinical Practice Guidelines in Oncology. *Journal of the National Comprehensive Cancer Network: JNCCN*. 2024;22:1. doi:10.6004/jnccn.2024.0029
2. Greten FR, Grivennikov SI. Inflammation and Cancer: triggers, Mechanisms, and Consequences. *Immunity*. 2019;51(1):27–41. doi:10.1016/j.immuni.2019.06.025
3. El Tekle G, Andreeva N, Garrett WS. The Role of the Microbiome in the Etiopathogenesis of Colon Cancer. *Annual Review of Physiology*. 2024;86(1):453–478. doi:10.1146/annurev-physiol-042022-025619
4. Oh A, Pardo M, Rodriguez A, et al. NF-κB signaling in neoplastic transition from epithelial to mesenchymal phenotype. *Cell Communication and Signaling: CCS*. 2023;21(1):291. doi:10.1186/s12964-023-01207-z
5. Manning BD, Toker A. AKT/PKB Signaling: navigating the Network. *Cell*. 2017;169(3):381–405. doi:10.1016/j.cell.2017.04.001
6. Xue G, Zippelius A, Wicki A, et al. Integrated Akt/PKB signaling in immunomodulation and its potential role in cancer immunotherapy. *Journal of the National Cancer Institute*. 2015;107(7):djv171–djv171. doi:10.1093/jnci/djv171
7. Huang JQ, Li H-F, Zhu J, et al. SRPK1/AKT axis promotes oxaliplatin-induced anti-apoptosis via NF-κB activation in colon cancer. *Journal of Translational Medicine*. 2021;19(1):280. doi:10.1186/s12967-021-02954-8
8. McIlwain DR, Berger T, Mak TW. Caspase functions in cell death and disease. *Cold Spring Harbor Perspectives in Biology*. 2015;7(4):a026716. doi:10.1101/cshperspect.a026716
9. Yu J, Li S, Qi J, et al. Cleavage of GSDME by caspase-3 determines lobaplatin-induced pyroptosis in colon cancer cells. *Cell Death & Disease*. 2019;10(193). doi:10.1038/s41419-019-1441-4
10. Shi L, Chen L, Jin G, et al. Si-Ni Decoction as a Potential Treatment for Ulcerative Colitis: modulation of Gut Microbiota and AKT1 Inhibition Through Network Pharmacology and in vivo Validation. *Journal of Inflammation Research*. 2025;18:6263–6280. doi:10.2147/jir.S516556
11. Chen J, Zheng X, Xu G, et al. Sini Decoction Inhibits Tumor Progression and Enhances the Anti-Tumor Immune Response in a Murine Model of Colon Cancer. *Combinatorial Chemistry & High Throughput Screening*. 2023;26(14):2517–2526. doi:10.2174/1386207326666230320103437
12. Liang B, Liang Y, Li R, Zhang H, Gu N. Integrating systematic pharmacology-based strategy and experimental validation to explore the synergistic pharmacological mechanisms of Guanxin V in treating ventricular remodeling. *Bioorganic Chemistry*. 2021;115:105187. doi:10.1016/j.bioorg.2021.105187
13. Szklarczyk D, Gable AL, Nastou KC, et al. The STRING database in 2021: customizable protein-protein networks, and functional characterization of user-uploaded gene/measurement sets. *Nucleic Acids Research*. 2021;49(D1):D605–d612. doi:10.1093/nar/gkaa1074
14. Piñero J, Bravo À, Queralt-Rosinach N, et al. DisGeNET: a comprehensive platform integrating information on human disease-associated genes and variants. *Nucleic Acids Research*. 2017;45(D1):D833–d839. doi:10.1093/nar/gkw943
15. Di H, Liu H, Xu S, Yi N, Wei G. Network Pharmacology and Experimental Validation to Explore the Molecular Mechanisms of Compound Huangbai Liquid for the Treatment of Acne. *Drug Design, Development and Therapy*. 2023;17:39–53. doi:10.2147/dddt.S385208
16. Doncheva NT, Morris JH, Holze H, et al. Cytoscape stringApp 2.0: analysis and Visualization of Heterogeneous Biological Networks. *Journal of Proteome Research*. 2023;22(2):637–646. doi:10.1021/acs.jproteome.2c00651
17. Jo S, Cheng X, Lee J, et al. CHARMM-GUI 10 years for biomolecular modeling and simulation. *Journal of Computational Chemistry*. 2017;38(15):1114–1124. doi:10.1002/jcc.24660
18. Taniguchi K, Karin M. NF-κB, inflammation, immunity and cancer: coming of age. *Nature Reviews. Immunology*. 2018;18:309–324. doi:10.1038/nri.2017.142
19. Bhat AA, Thapa R, Afzal O, et al. The pyroptotic role of Caspase-3/GSDME signalling pathway among various cancer: a Review. *International Journal of Biological Macromolecules*. 2023;242:124832. doi:10.1016/j.ijbiomac.2023.124832
20. Yu JS, Cui W. Proliferation, survival and metabolism: the role of PI3K/AKT/mTOR signalling in pluripotency and cell fate determination. *Development (Cambridge, England)*. 2016;143(17):3050–3060. doi:10.1242/dev.137075
21. Okon IS, Zou MH. Mitochondrial ROS and cancer drug resistance: implications for therapy. *Pharmacol Res*. 2015;100:170–174. doi:10.1016/j.phrs.2015.06.013
22. Jia Q, Wang B, Shu YH, et al. The structure of glyuranolide, a new triterpene of Glycyrrhiza uralensis Fisch. *Acta Pharmaceutica Sinica*. 1989;24(5):348–352.